Computers in Biology and Medicine 134 (2021) 104480

Contents lists available at ScienceDirect

Computers in Biology and Medicine

journal homepage: www.elsevier.com/locate/compbiomed

Ex-post correction of pacemaker mode switch episodes in undersensed atrial fibrillation

Jesús Fernández [a], Luciano Sánchez [b,*], David Calvo [c], Julián Velasco [d]

[a] Electrical and Electronics Engineering Department, Oviedo University, 33203, Gijón, Spain
[b] Computer Science Department, Oviedo University, 33203, Gijón, Spain
[c] Arrhythmia Unit, Cardiology Department, Hospital Universitario Central de Asturias, Instituto de Investigación Sanitaria Del Principado de Asturias (ISPA), 33011, Oviedo, Spain
[d] Mathematics Department, Oviedo University, 33000, Oviedo, Spain

ARTICLE INFO

Keywords:
Arrhythmia
Expectation-maximimization
Cardiac implantable electronic devices

ABSTRACT

Background: Information about short Atrial Fibrillation (AF) episodes can be gathered from the diagnostic records of cardiac implantable electronic devices (CIEDs). CIEDs are not accurate when detecting short arrhythmia episodes. The correlation between mode switching events and AF episodes is significant for long events but prone to errors for short episodes.
Methods: Expectation-maximization algorithms are used to estimate the parameters of a mathematical model from a list of AF episodes produced by the CIED. The durations of some of the episodes may be missing. Abnormal mode changes are detected and short episodes are joined into longer events when appropriate. The proposed method does not require that the sensitivity parameters of the device are altered. Post-processing of the data is limited to the detection of false negatives, thus paroxysmal arrhythmia diagnostic evaluations are safer.
Results: A three year-long study was carried out with patients with dual-chamber pacemakers (PM) at the Hospital Universitario Central de Asturias (Spain) between 2012 and 2015. The number of patients in which the proposed algorithm altered the final histogram was 40 out of 76. On average, the algorithm removes 2.79% of episodes shorter than 1 min in length and finds that 1% of the previously unaccounted episodes are longer than 30 min, of which 16% are longer than 24 h.
Conclusion: The method is stable and guarantees that long arrhythmia episodes are never eliminated, and at the same time it is the most similar to the human expert in finding new long episodes.

1. Introduction

Atrial fibrillation (AF) is the most common permanent tachycardia in the adult population. The estimated prevalence of AF in adults is 2–4% and a 2.3-fold rise is expected [5,13]. AF can be divided into three categories: paroxysmal, persistent and permanent. Paroxysmal atrial fibrillation (PAF) episodes are self-terminating and last less than seven days [13]. PAF episodes can, in turn, be classified into two rhythm patterns: the *staccato* subtype, characterized by many short episodes with small separation, and the *legato* subtype, with a few, well separated long events [24]. There is a wide consensus about the inherent risk in the long episodes, but the shorter episodes have not been regarded as important until recent times [9]. Short episodes (less than 5 min) are often excluded, to avoid oversensing [15].

Information about short episodes can be gathered from the diagnostic records of cardiac implantable electronic devices (CIEDs) [10,17], including pacemakers and implantable defibrillators. CIEDs have a bipolar sensing lead in the atrial chamber and analyze the atrial rhythm to detect atrial tachycardia and, in certain cases AF, for arrhythmia monitoring [22]. To obtain accurate records, proper implementation and adjustments are required: an appropriate sensitivity and optimal postventricular recovery periods (post-ventricular atrial blanking and refractory periods). The reason is that the two periods interact. Furthermore, AF detection algorithms have manufacturer-dependent limitations [13], with false positives due to over-detection or far-field (FF) and false negatives due to underdetection. For appropriate decision making it is critical to ascertain the duration of the AF episodes, as clinicians rely on duration of device-detected AF as an indicator of the

* Corresponding author.
E-mail address: luciano@uniovi.es (L. Sánchez).

https://doi.org/10.1016/j.compbiomed.2021.104480
Received 29 December 2020; Received in revised form 24 April 2021; Accepted 6 May 2021
Available online 23 May 2021

patient risk [23].

According to Refs. [16,20], Atrial Model Switching (AMS) activations are generally reliable (the number of false positives is low) but AMS deactivations are not (high fraction of false negatives). This behaviour is admitted because it does not pose a risk to the patient: if a spurious AMS deactivation is issued while an AF episode is taking place, the CIED resumes the monitoring of the atrial frequency and issues a new AMS activation in seconds. In any case, this implies that:

1. The registered durations of certain AF episodes (those with unreliable AMS deactivations) are missing in the CIED register.
2. A long episode may be perceived as a sequence of short episodes [16].

When episodes of mode switching stored in pacemaker diagnostics were correlated to surface ECGs and Holter monitors [20], it was found that, if the pacemaker operates with its standard settings, up to 17% of false negatives were possible (8 of 46 patients). In Ref. [16] a similar fraction of false negatives was obtained with 6-min episodes. Both studies conclude that the correlation between mode switching events and AF episodes is significant for long events but prone to errors for short episodes.

The usefulness of CIEDs as sensors of AF in patients of the *staccato* subtype and other specific changes, such as ablation failures, is therefore limited. However, there are studies such as [21] showing that even 30 s episodes are relevant, and that small differences in the AF episode lengths affect the perceived incidence of AF (and AF ablation success). Thus, there is an interest in procedures that increase the accuracy of implantable electronic devices when measuring the length of short AF events.

This paper presents a method for improving the accuracy of measurements of AF episodes obtained from CIED records. Expectation-maximization (EM) algorithms for coarse data are applied to post-process the list of AF episodes produced by the CIED. Short episodes are joined into longer events when appropriate. Being an *ex-post* procedure, the existing sensitivity parameters of the CIED need not to be altered. Furthermore, the post-processing is safe in the sense that it is limited to the detection of false negatives. The mean duration of the postprocessed episodes will always be equal or higher than that of the raw episodes. This application of EM algorithms is novel for two reasons:

1. It is stable and guarantees that long arrhythmia episodes are never eliminated.
2. According to our experimentation, it is more effective than machine learning-based alternatives for finding long undetected episodes.

This paper is organized as follows: The datasets used in this study are described in Section 2. In Section 3 a mathematical model of the CIED is introduced. In Section 4 an algorithm for fitting this model to a possibly incomplete list of AF episodes data is derived. In Section 5 an empirical study is carried out where the procedure is tested in simulated data with known properties, and in a sample of 76 patients. The outcome of the methodology is detailed in three representative patients. In Section 6 concluding remarks are made and future work is suggested.

2. Description of the datasets

A three-year-long study was carried out with 76 patients with dual-chamber pacemakers (PM) at the *Hospital Universitario Central de Asturias* (Spain) between 2012 and 2015. Patients have Atrioventricular Block (AVB) in 57 of 76 cases and Sinus Node Disease (SND) in 19 of 76. Patients were checked according to the usual clinical practice of the hospital, which was annually unless a problem arose. Clinical data is downloaded from the memory of the device, which has the capacity to store dates and durations of the last 27 episodes. The device is capable of producing a histogram of the durations of the episodes and also captures 15 second-long intracardiac electrograms (iECGs) for the stored episodes. These iECGs correspond to the beginning of the arrhythmia, and include 10 s prior to activation. A total of 1894 events with captured iECG were recorded.

3. Dynamic model of AMS activations and deactivations

Registering a long episode as a sequence of short episodes does not pose any safety concerns, because the time between each AMS deactivation and its subsequent AMS activation is short. However, the histogram of durations changes when a long event is divided into short events. Given that these histograms are part of the diagnostic evaluation of PAF in relation to anticoagulation, this paper defends the view that uncorrected histograms may give an overly optimistic view of the patient's condition.

A dynamical model of AMS activations and deactivations is adopted that considers the probability that the CIED detection algorithm generates false negatives [6]. The parameters defining the model will be estimated by an algorithm that maximizes the likelihood of the measured AF episode lengths (see Section 4). Each of the AMS changes will be labelled as "normal" or "artifact", so artifacts can be removed and chains of AF episodes with removed AMSs are joined into a single episode.

Fig. 1 depicts the states and transitions of the proposed model. This is a continuous time Markov model [18] with three states: (1) True Negative (no arrhythmia), (2) Positive (AF episode) and (3) False Negative (artifact). The third state is associated with those cases where the CIED has detected a non-existent end of the AF episode and an AMS deactivation/AMS activation pair is issued.

There are AMS events (activations) in transitions from True and False Negatives to Positive. Times at states "Positive", "False Negative" and "True Negative" follow exponential distributions with parameters λ_{A}, λ_{GA} and λ_{NA}, respectively. The probability that a transition happens between states "Positive" and "False Negative" is p_{AG}, and the probability of a transition between "Positive" and "True Negative" is $p_{\mathrm{AN}} = 1 - p_{\mathrm{AG}}$. In the following we will assume that the time it takes for the algorithm to re-detect an arrhythmia after a premature exit is negligible:

$$(\mathrm{H1}): \quad \frac{1}{\lambda_{\mathrm{GA}}} \approx 0. \tag{1}$$

Therefore, the time between any two consecutive AMS activations belongs to one of the following alternatives:

- *Positive* → *True Negative* → *Positive* (T1). The expected time lapse between two AMS events is

$$\frac{1}{\lambda_{\mathrm{AN}}} + \frac{1}{\lambda_{\mathrm{NA}}}. \tag{2}$$

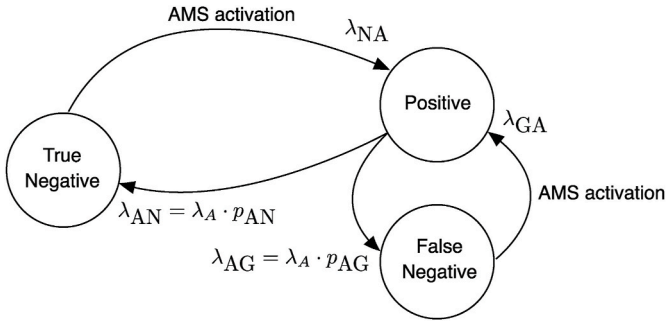

Fig. 1. State diagram of the dynamical model of the beginning of the CIED detection algorithm [6].

- Positive → False Negative → Positive, that will be simplified to *Positive* → *Positive* (T2), with expected duration

$$\frac{1}{\lambda_{AG}}, \tag{3}$$

where $\lambda_{AN} = \lambda_A \cdot p_{AN}$ and $\lambda_{AG} = \lambda_A \cdot p_{AG}$.

4. Proposed methodology

The purpose of the methodology introduced in this section is to separate the time intervals between AMS activations into two categories: full AF episodes (T1, alternative "Positive" to "True Negative") and false short episodes (T2, alternative "Positive" to "Positive"), in order to remove this second type of AMS events from the sequence and recalculate the histogram of durations.

The parameters of the model are estimated with an Expectation-Maximization algorithm [3]. Intervals are labelled as ordinary (type T1) or artifacts (T2) according to the posterior likelihood of either alternative. There is a very extensive literature about parameter estimation in Markov models (see Ref. [19] for a recent review) but it must be said that this is not a conventional problem because transitions from "Positive" to "True Negative" and "False Negative" may not be logged in the CIED record. The model parameters must be estimated with partially missing or *coarse* data [7,11,12,14], consisting of a mixture of either the sum of the times of two transitions (T1) or one transition plus a negligible time (T2). A specific estimation methodology will be developed in the remainder of this section.

4.1. Probability distribution of the intervals

According to the proposed model, there are two possible paths between AMS activations (recall Fig. 1): (T1) Positive → True Negative → Positive and (T2) Positive → False Negative → Positive. The time spent on the path (T1) is the sum of two random variables with exponential probability distributions, which is a hypoexponential distribution. The time spent on the path (T2) can be approximated by an exponential distribution, because the transition from False Negative to Positive is very fast.

The hypoexponential distribution depends on two parameters, λ_{AN} and λ_{NA}. The exponential distribution depends on one parameter, λ_{AG}. Estimating λ_{AN}, λ_{NA} and λ_{AG} from data is not trivial if some of the durations of the AF episodes are not registered by the CIED (that is, when some of the measurements of the times between the states "Positive" and "True Negative" are missing).

We will denote by $f(t|\lambda)$ the probability density function of an exponential distribution with rate parameter λ. $f(t|\lambda_1, \lambda_2)$ is the probability density function of a hypoexponential distribution with rates λ_1 and λ_2. The probability distribution of the time between two episodes is a weighted combination of the respective distributions of the elapsed times in paths (T1) or (T2), and these weights are the probabilities of taking each path (see Appendix A for the derivation of this formula):

$$f_T(t) = p_{AG} f(t|\lambda_A) + p_{AN} f(t|\lambda_A, \lambda_{NA}) \tag{4}$$

4.2. Numerical algorithm

The parameters defining the probability distribution in Eq. (4), are p_{AG}, p_{AN}, λ_A and λ_{NA}, with $\lambda_{AN} = \lambda_A \cdot p_{AN}$, $\lambda_{AG} = \lambda_A \cdot p_{AG}$ and $p_{AN} = 1 - p_{AG}$. Once these parameters are estimated, the probabilities that an interval between two episodes matches paths (T1) or (T2) are inmediately obtained. If the probability of path (T2) is greater than that of path (T1), then the first AF episode is spurious and can be eliminated.

If this estimate could be solved by finding the global minimum of the likelihood function (e.g., by a descent algorithm) it would not be necessary to develop an algorithm of our own. In Appendix B we show that this is not possible, since the likelihood function has several minima even in the particular case where all paths are of type (T1) and all durations are unknown. For this reason, we propose to solve the optimization problem using an EM algorithm. In Appendix E we define such an algorithm for the same simplified case in which all paths are of type (T1) and the durations of all episodes are unknown, and in Appendix F we derive the algorithm for the general case in which part of the durations are known and part are unknown. In Appendix I we show that the proposed algorithm converges to the desired solution.

A pseudocode summarizing all the steps of the proposed algorithm is shown in Fig. 2. The inputs to the algorithm are the times between episode onsets (Δ), the initial estimates of λ_A, λ_{NA} and p_{AN} obtained using the heuristic in Appendix J, and the episode durations. The results of the algorithm are the final estimates of λ_A, λ_{NA} and p_{AN}, and a vector Γ_1. The interval between two episodes is marked as spurious (T2) when the corresponding component of the vector Γ_1 is greater than 0.5. The Python source code of this algorithm can be downloaded from the "Mendeley Data" dataset indicated in the body of reference [8].

5. Empirical study

This section contain two sets of empirical studies, serving two purposes: (a) validating the methodology in datasets with known properties and (b) illustrating the behaviour of the algorithm in representative cases, with emphasis in the changes in the diagnostic evaluation of PAF.

5.1. Simulated data with known properties

Wineiger's work [24] was taken as a reference for choosing the parameters of the simulations. A database comprising 13,000 patients and more than 1 million of AF episodes was studied, and it was found that the median of the number of episodes per day is 1.21 and the mean duration of an episode is 16.6 min. According to our own experience, each patient will be associated with a list comprising between 100 and 500 CIED logs. The model parameters needed for reproducing Wineiger's statistics are therefore

$$\frac{1}{\lambda_{AN}} = 16.6 \text{ minutes} = 996 \text{ seconds}.$$

$$\frac{1}{\lambda_{NA}} = \frac{24*60}{\log(2)*1.21} \approx 1717 \text{ minutes}.$$

The input to the EM algorithm is a Monte Carlo generated list of "AMS" events and a fraction f of the "END AF" events, using the mentioned parameters. The initial coefficients for starting the EM algorithm are obtained by means of a heuristic that is described in Appendix J. The EM algorithm is stopped after 500 generations.

From a statistical point of view, the simulations are compatible with the experimental measurements of the duration and distance between events that are shown in the next section. The simulated data are relevant because, unlike the case of the real data, the parameters p_{AG}, p_{AN}, λ_A and λ_{NA} are known and therefore we can check that the algorithm has converged to the correct solution. Furthermore, we can introduce different percentages of missing durations and check to what extent the limits of the CIED storage capacity affect its usefulness as a diagnostic tool. In this sense, the results shown in this section are an optimistic estimate of the possibilities of the proposed methodology: in real patients the fit of the data to the model will not be perfect and therefore to the estimation errors shown in this section the effect of discrepancies between reality and the model must be added.

Note that the Wineinger data are obtained by automatic procedures and for this reason the number of short AF episodes is probably downward biased, as is the case with our own data. This should not affect the conclusions of the simulation, because in the synthetic data it is known when the event is spurious and when it is real. In any case, the percentages shown in the tables discussed below could be subject to variations if the values of λ_{AN} y λ_{NA} had been chosen differently.

```
def EM(Δ,λ1,λ2,τ,duration):
    repeat
        β1=(1 − τ) · exp(−λ2 · Δ) · integral1(λ2 − λ1, Δ) · λ1 · λ2/mixed(λ1, λ2, τ, Δ)
        β2=(1 − τ) · exp(−λ2 · Δ) · integral2(λ2 − λ1, Δ) · λ1 · λ2/mixed(λ1, λ2, τ, Δ)
        Γ1=τ · exponential(λ1, Δ)/mixed(λ1, λ2, τ, Δ)
        Γ2=(1 − τ) · hypoexponential(λ1, λ2, Δ)/mixed(λ1, λ2, τ, Δ)
        Γ1[duration > 0] = 0; Γ2[duration > 0] = 1
        β1[duration > 0] = duration[duration > 0]
        β2[duration > 0] = (Δ − duration)[duration > 0]
        Γ1[duration == Δ] = 1; Γ2[duration == Δ] = 0
        β1[duration == Δ] = 0; β2[duration == Δ] = 0
        λ1^new=len(Δ)/∑(Γ1Δ + β1)
        λ2^new=∑Γ2/∑β2
        τ^new = (1/∑Γ2)/((1/∑Γ1) + 1/∑Γ2)
        error=|λ1−λ1^new| + |λ2−λ1^new| + |τ − τ^new|
        λ1=λ1^new
        λ2=λ1^new
        τ=τ^new
    until the limit of iterations is reached or the error falls below a threshold
    return λ1,λ2,τ,β1,β2,Γ1,Γ2


def integral1(a,x):
    return select([a==0,a≠0], [x^2/2, (1 + (ax − 1)e^ax)/a^2])

def integral2(a,x):
    return select([a==0,a≠0], [x^2/2, −(1 + ax − e^ax)/a^2])

def mixed(λ1,λ2,τ,x):
    return τ · exponential(λ1, x) + (1 − τ) ∗ hypoexponential(λ1, λ2, x)
```

Fig. 2. Pseudocode of the proposed algorithm. The inputs to the EM function are the times between episode onsets (Δ), the initial estimates of λ_1, λ_2 and τ obtained using the heuristic in Appendix J, and the episode durations (unknown durations are represented by the value 0). The results of the algorithm are the final estimates of λ_1, λ_2 and τ, and the vectors β_1, β_2, Γ_1 and Γ_2. The interval between two episodes is marked as spurious (T2) when the corresponding component of the vector Γ_1 is greater than 0.5.

Simulation results are shown in Tables 1–4. The purpose of the simulations is to test the best-case behavior of the proposed algorithm under different conditions. First, the combined effects of insufficient CIED storage capacity (parameter *f*) with the unreliability of detecting the output of an episode (parameter τ), for patients with a short history (100 episodes), are shown. Second, the experiments are repeated five times, for the same value of τ, to check the variance of the results. Both tables are repeated for long histories (500 episodes).

Row labels $f = 0, f = 0.2, f = 0.4, f = 0.6, f = 0.8$ and $f = 1$ indicate the fraction of coarse data (missing AF episode lengths). Column labels $\tau = 0, \tau = 0.2, \tau = 0.4, \tau = 0.6$ and $\tau = 0.8$ indicate the fraction of false negatives, $\tau = 0$ being the least favourable case (i.e $\tau = 0$ means that none of the AF episode lengths are available). Each cell in the tables contains two numbers: the estimation in seconds of the duration of an AF episode and the relative error of the estimation with respect to the sample values. Tables 1 and 2 are results for simulated CIED records comprise 100 samples, and Tables 3 and 4 are estimations for 500 samples.

It must be noted that the EM algorithm does not converge to population values, but to sample values, that is to the sample means when $f =$

Table 1
Simulations with simulated data comprising 100 episodes. Rows: proportion *f* of coarse data. Columns: proportion τ of false negatives (premature detections of the end of AF episodes). Each cell contains the estimated AF episode length (in seconds) and the relative error percentage with respect to sample values.

100 samples	$\tau = 0$	$\tau = 0.2$	$\tau = 0.4$	$\tau = 0.6$	$\tau = 0.8$
$f = 0$	964	1024	874	1312	813
$f = 0.2$	942 [1%]	988 [4%]	901 [3%]	1345 [2%]	824 [1%]
$f = 0.4$	977 [1%]	1015 [1%]	892 [2%]	1285 [2%]	813 [0%]
$f = 0.6$	936 [3%]	1203 [17%]	891 [2%]	1389 [6%]	824 [1%]
$f = 0.8$	821 [14%]	1022 [0%]	881 [1%]	1416 [8%]	821 [1%]
$f = 1$	No	601 [41%]	820 [6%]	1581 [20%]	812 [0%]

Table 2
Variability associated to sampling: First row: sample values (estimations without coarse data) for five different simulated samples comprising 100 episodes each and $\tau = 0.4$. Rows second to sixth: EM estimations on the same samples and a fraction *f* of coarse data. Each cell contains the estimated AF episode length and the relative error percentage with respect to sample values. All times are measured in seconds.

100 samples	Sample #1	Sample #2	Sample #3	Sample #4	Sample #5
$f = 0$	962	1339	1029	983	1083
$f = 0.2$	936 [3%]	1228 [4%]	967 [6%]	1030 [5%]	1053 [3%]
$f = 0.4$	982 [2%]	1258 [6%]	924 [10%]	989 [1%]	982 [9%]
$f = 0.6$	930 [3%]	1327 [1%]	921 [10%]	797 [19%]	1000 [8%]
$f = 0.8$	937 [3%]	1376 [3%]	851 [17%]	814 [17%]	1035 [4%]
$f = 1$	844 [12%]	1094 [18%]	903 [12%]	824 [16%]	923 [15%]

Table 3
Simulations with simulated data comprising 500 episodes. Rows: proportion f of coarse data. Columns: proportion τ of false negatives (premature detections of the end of AF episodes). Each cell contains the estimated AF episode length and the relative error percentage with respect to sample values. All times are measured in seconds.

500 samples	$\tau = 0$	$\tau = 0.2$	$\tau = 0.4$	$\tau = 0.6$	$\tau = 0.8$
$f = 0$	1018	968	1028	875	1060
$f = 0.2$	985 [3%]	959 [1%]	1033 [0%]	889 [2%]	1057 [0%]
$f = 0.4$	966 [5%]	953 [2%]	1026 [0%]	892 [2%]	1081 [2%]
$f = 0.6$	947 [7%]	930 [4%]	1022 [1%]	904 [3%]	1096 [3%]
$f = 0.8$	914 [10%]	898 [7%]	1016 [1%]	936 [7%]	1092 [3%]
$f = 1$	4525 [340%]	791 [18%]	1093 [6%]	971 [11%]	1118 [5%]

Table 4
Variability associated with sampling: First row: sample values (estimations without coarse data) for five different simulated samples comprising 500 episodes each and $\tau = 0$. Rows second to sixth: EM estimations on the same samples and a fraction f of coarse data. Each cell contains the estimated AF episode length and the relative error percentage with respect to sample values. All times are measured in seconds.

500 samples	Sample #1	Sample #2	Sample #3	Sample #4	Sample #5
$f = 0$	1057	1000	889	1068	1007
$f = 0.2$	1070 [1%]	1022 [2%]	876 [1%]	1073 [0%]	1025 [2%]
$f = 0.4$	1076 [2%]	1033 [3%]	848 [5%]	1114 [4%]	981 [3%]
$f = 0.6$	1142 [8%]	1043 [4%]	871 [2%]	1140 [7%]	1027 [2%]
$f = 0.8$	1196 [13%]	1006 [1%]	851 [4%]	1252 [17%]	1048 [4%]
$f = 1$	1057 [85%]	4356 [335%]	1446 [62%]	668 [37%]	599 [40%]

0. This is demonstrated in Appendix I, where it is shown that the critical points of the likelihood function fulfill that $\frac{1}{\lambda_1} + \frac{1-\tau}{\lambda_2}$ coincide with the sample mean, which is not the population mean.

For large samples, the proportion of false negatives, the average length of an AF episode and the average delay between the end of an episode and the next AMS event will be near the theoretical (population) values τ, $\frac{1}{\lambda_{AN}}$ and $\frac{1}{\lambda_{NA}}$ respectively, but the differences may be of importance for small samples. According to our experimentation, for simulations comprising 100 events, the differences between the theoretical times and the Monte Carlo simulated times can as high as 30%. For simulations of size 500, these differences differ at most by 10%. We may reduce these differences by increasing the sample size, but that would not be realistic because we rarely find CIED records longer than 500 episodes.

It must be noted that the errors in the EM estimation are expected to be of the same order as the variability associated with sampling. This variability is illustrated in Table 2. The first row contains sample values (estimations without coarse data) for five different simulated samples comprising 100 episodes each and $\tau = 0.4$. The other rows in the table are EM estimations on the same samples when there is a fraction f of coarse data, showing a good resilience for samples with a high percentage of missing AF episode lengths.

Lastly, in Table 4 the least favourable case is depicted: a sample without premature ends of AF episodes ($\tau = 0$) and 500 events is analyzed. Although the approximation is good when the number of coarse intervals is moderately high ($f = 0.6$), the last row of this table shows that the algorithm does not converge to the desired values when none of the AF episode lengths and at the same time none of the episode lengths are available. In this particular case, the specific EM algorithm for the hypoexponential case (see Section E) should be used.

5.2. Comparison with other methods

In order to compare the proposed method with different alternatives in the literature, an expert has examined the iECGs of the episodes of 76 patients and manually labelled the false arrhythmia episodes. The raw histograms downloaded from the PMs have been compared with the manually corrected histograms in the first place, then with histograms processed by the proposed method and finally with histograms corrected by a selection of machine learning algorithms that have been employed in the literature to process digital cardiac arrhythmia data [2].

The means of the bar heights of the raw PM histograms, the expert corrections to these values and the results of four different machine learning algorithms are shown in Table 5. There are two numbers in each cell of the table. The first number is the mean height of each bar of the corrected histogram for each of the studied corrections. The second number (in parentheses) is the difference between the corrected value and the raw PM value. Anomalous numbers have been marked in bold. These numbers are downward corrections of the fraction of arrhythmias with clinical interest; that is, the methods with bold values produced a potentially unsafe correction of some patients' histograms. SVC is a support vector machine, MLP is a neural network, KNN is the k-nearest neighbour algorithm and ADA is the Adaboost classifier [1]. The input variables of the training sets of the classifiers comprise the episode length and the time between the current episode and the preceding one. The outputs are the labels provided by the expert for each episode. Columns SVC, MLP, KNN and ADA contain test results obtained by 10-fold cross validation: each classifier was trained on 90% of the data and evaluated on the remaining 10%, and the process was repeated 10 times for each method. It is important to say that the proposed method does not use human-labelled training data and relies solely in the dynamic model introduced before.

Note that the expert has labelled a high number of short episodes (less than 1 min) as false negatives. He has also combined the episodes before and after these false negatives, so that the fraction of long arrhythmias (greater than 12 h) is higher. In some cases, he has also detected that an apparently long arrhythmia is a false episode because of far-field problems, so some arrhythmia episodes with duration between 6 and 12 h were removed. The proposed method is stable and will not remove these long episodes, because it is ensured that the mean duration of the processed episodes must be equal to or greater than the original mean duration. Despite this, the number of post-processed arrhythmias lasting 24 h or more is higher than the alternatives. Finally, let us note that neither statistical classifiers nor those based on machine learning maintain this stability property, i.e., it is possible that the modified histogram may have a shorter mean arrhythmia duration than the original histogram.

5.3. Representative cases

The data described in Section 2 have been analyzed by a technical specialist in the diagnosis of arrhythmia, who has selected three representative patients for a detailed explanation. In the first of the selected cases, the post-processed episodes do not alter the original measurement of the PM. In the other two cases the algorithm has made a correction with possible diagnostic significance.

It must be pointed out that the number of patients in which the proposed algorithm altered the final histogram was 40 out of 76. This means that, in the conditions of this study, PMs histograms of durations are not reliable in more than half (53%) of cases, underlining the importance of this study.

Table 5
Comparison of different arrhythmia histogram correction strategies. All values in the table are percentages. The second column comprises the raw PM percentages and the following columns are, respectively, the corrections applied by an expert, the automatic method proposed in this work and a selection of statistical and artificial intelligence-based classifiers: SVC is a Support Vector Classifier, MLP is a three layer Neural Network, KNN is the k-nearest neighbours algorithm and ADA is an Adaboost ensemble of classifiers. There are two numbers in each cell of these last columns. The first number is the mean height of each bar of the corrected histogram for each of the studied corrections. The second number (in parentheses) is the difference between the corrected value and the raw PM value. The proposed method is stable and ensures that long arrhythmia episodes are never removed, and at the same time is the nearest to the human expert in long episodes. The methods with bold values produced a potentially unsafe correction of some patients' histograms.

Length	PM	Expert	This method	SVC	MLP	KNN	ADA
0–1 min	61.77	52.44 (−9.33)	58.97 (−2.79)	61.42 (−0.35)	61.07 (−0.69)	61.57 (−0.19)	61.17 (−0.60)
1–5 min	14.66	13.94 (−0.72)	15.95 (+1.29)	14.53 **(-0.13)**	15.10 (+0.44)	14.51 **(-0.16)**	14.98 (+0.32)
5–15 min	5.99	5.15 (−0.84)	6.26 (+0.27)	6.15 (+0.16)	5.96 **(-0.03)**	6.22 (+0.23)	6.11 (+0.12)
15–30 min	4.02	3.21 (−0.81)	4.23 (+0.21)	4.12 (+0.10)	4.11 (+0.09)	4.04 (+0.02)	4.11 (+0.09)
30 min - 1 h	3.25	8.95 (+5.70)	3.94 (+0.69)	3.31 (+0.06)	3.29 (+0.05)	3.37 (+0.12)	3.28 (+0.03)
1 h–3 h	3.54	5.09 (+1.55)	3.65 (+0.10)	3.55 (+0.00)	3.59 (+0.05)	3.57 (+0.02)	3.56 (+0.02)
3 h–6 h	1.75	4.02 (+2.27)	1.78 (+0.03)	1.77 (+0.02)	1.68 **(-0.07)**	1.71 **(-0.04)**	1.65 **(-0.10)**
6 h–9 h	0.81	0.66 (−0.15)	0.82 (+0.02)	0.86 (+0.05)	0.90 (+0.09)	0.74 **(-0.06)**	0.71 **(-0.10)**
9 h–12 h	0.22	0.15 (−0.07)	0.23 (+0.01)	0.26 (+0.04)	0.23 (+0.01)	0.23 (+0.01)	0.26 (+0.04)
12 h–24 h	0.98	1.07 (+0.09)	1.00 (+0.02)	0.94 **(-0.04)**	1.01 (+0.04)	0.94 **(-0.03)**	1.05 (+0.07)
> 24 h	3.02	5.33 (+2.31)	3.17 (+0.16)	3.10 (+0.08)	3.05 (+0.04)	3.10 (+0.08)	3.12 (+0.11)

5.3.1. *Patient A: unaltered histogram*

This patient (see Fig. 3) is representative because the expert did not detect inconsistencies in the raw durations (blue histogram). The post-processed durations (orange histogram) evince that the algorithm is safe in terms of the correct diagnosis of paroxysmal atrial fibrillation, because the post-processed episodes have durations equal to or greater than the raw episodes.

5.3.2. *Patient B: false negatives*

There is a high number of false negatives in Patient B, and also a high number of episodes without attributed duration. The iECG of one of these false negatives is depicted in Fig. 4. The PM has detected a spurious end of the AF episode (red vertical line, pacing in dual chamber or DDD mode) and a new AF event was issued 7 s later (blue vertical line, change to atrioventricular sequential dual-chamber inhibited rate-responsive nontracking but atrial sensing mode or DDIR pacing). The post-processed histogram (see Fig. 5) shows that these false negatives have been correctly identified and removed, thus the bar in 0–1 min disappears and the mode of the post-processed distribution becomes 1–5 min.

5.3.3. *Patient C: wrong maximum duration*

Patient C (see Fig. 6) is representative because the raw data indicates that the longest AF events are of 5–15 min, which is wrong. The reasons can be explained with the help of the iECG in Fig. 7. The PM correctly activates the AMS (first vertical blue line) when it detects a high atrial

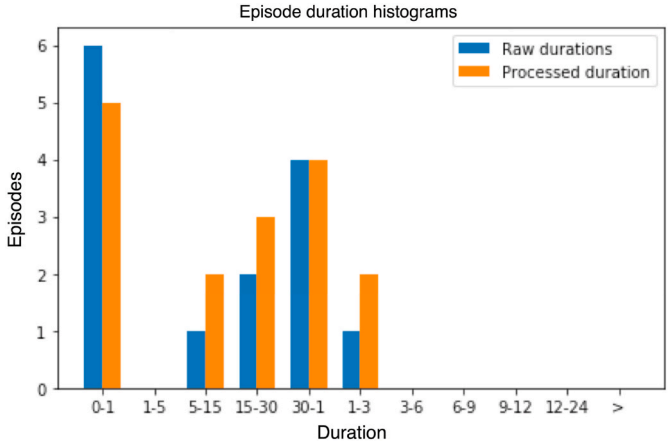

Fig. 3. Patient A: unaltered histogram. Durations are 0–1 min, 1–5 min, 5–15 min, 15–30 min, 30min-1h, 1–3 h, 3–6 h, 6–9 h, 9–12 h, 12–24 h and greater than 24 h.

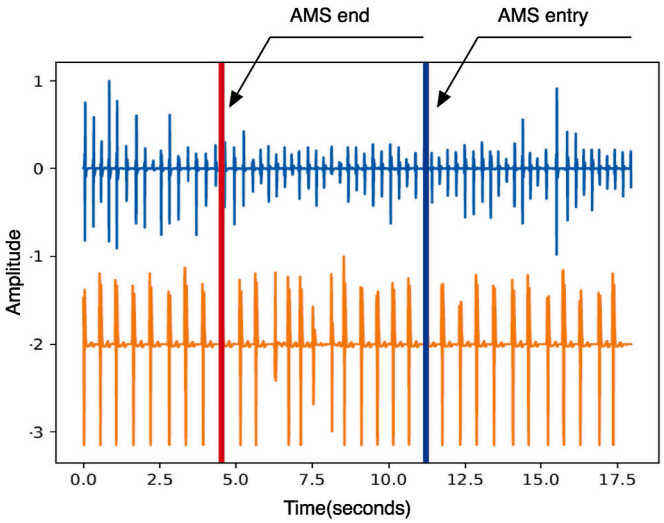

Fig. 4. Patient B: iECG of a false negative. The PM has detected an spurious end of the AF episode that has been followed by a reentrance 7 s later. Blue channel: atrium. Orange channel: ventricle. Red vertical line: DDD pacing. Blue vertical line: DDIR pacing.

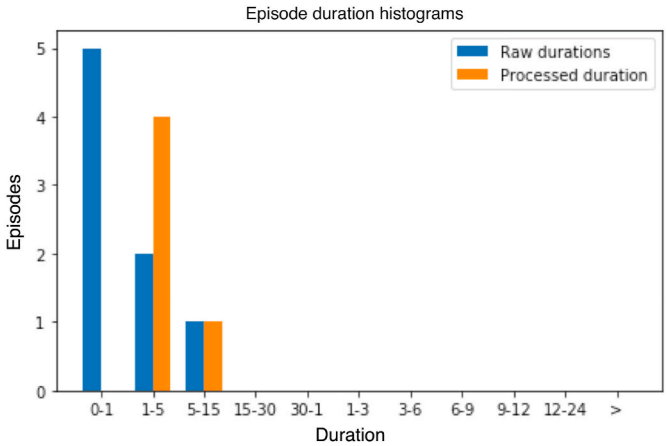

Fig. 5. Patient B. The histogram is altered by the removal of the short episodes (bar in 0–1 min). Durations are 0–1 min, 1–5 min, 5–15 min, 15–30 min, 30min-1h, 1–3 h, 3–6 h, 6–9 h, 9–12 h, 12–24 h and greater than 24 h.

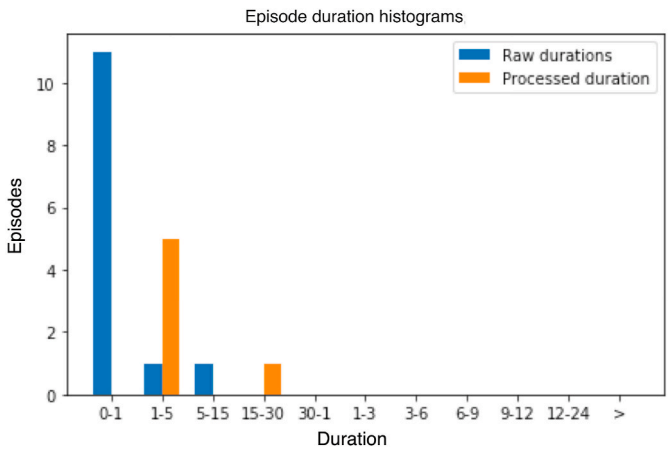

Fig. 6. Patient C. The histogram is altered by the removal of the short episodes (bar in 0–1 min) and a new bar appears for duration 15–30 which may be relevant for the diagnostic. Durations are 0–1 min, 1–5 min, 5–15 min, 15–30 min, 30min-1h, 1–3 h, 3–6 h, 6–9 h, 9–12 h, 12–24 h and greater than 24 h.

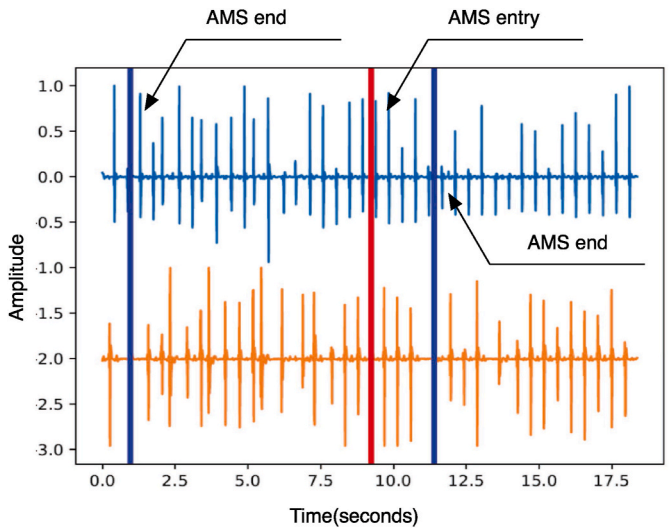

Fig. 7. Patient C. The PM correctly activates the AMS (first vertical blue line) when it detects a high atrial frequency, but after a few seconds it is deactivated (vertical red line), although the arrhythmia continues to be in progress. A few seconds later is detected again (second blue line). Blue channel: atrium. Orange channel: ventricle. Red vertical line: DDD pacing. Blue vertical line: DDIR pacing.

frequency, but after a few seconds it is deactivated (vertical red line), although the arrhythmia is still in progress. A few seconds later the AF episode it is detected again (second blue line) as if it was a new event. After processing, the number of long episodes is higher because some episodes were fused and some short episodes (0–1min) were removed. Note that, unlike patient B, in this case a new bar appears in the duration 15–30 min, where there were no previously recorded events. This new bar could be diagnostically relevant.

6. Concluding remarks and future work

Given the storage limitations of the CIEDs, it is not always possible to verify the stored duration of an AF episode with its corresponding iECG. There are cases in which the histogram of durations of a patient is the only available information. However, episode lengths were shown to be unreliable: the histograms were overly optimistic in more than half of the cases in this study. And even if EGM are available for visual analysis and review, this could be very tedious in clinical practice if the number of episodes is large. So, automatic algorithms providing reliable metrics and histograms on AF duration are clearly desirable from a clinical perspective.

A method has been proposed to post-process these histograms, removing false negatives and fusing short episodes together. The methodology consists in fitting a mathematical model to the list of the dates of the AF events and at the same time to a partially incomplete list of episode durations. A new expectation-maximization algorithm for coarse data was developed, and it was shown that the proposed algorithm converges to the desired solution in a wide range of conditions. The proposed method does not require altering the functioning parameters of the CIED, and post-processed histograms have an increased average episode length. The properties of the proposed procedure have been demonstrated first, validated with simulated data with known properties in the second place, and applied to data collected in a three-year long study finally.

In future studies we intend to extend this analysis to the investigation of the long-term evolution from paroxysmal to permanent arrhythmia. In its current state, the algorithm assumes that the parameters defining the duration of the arrhythmia have not changed during the study, and also that the arrhythmia is of the paroxysmal type. However, it is possible to extend the model so that the parameters λ_{NA} and λ_{AN} are functions of time. In this case, the extended algorithm could detect the point of change between the conditions that in clinical practice are associated with paroxysmal and permanent arrhythmias. The cases where this future EM algorithm would converge to the desired solution in the time-varying model will be established in future studies.

Acknowledgements

This work has been funded by the Ministry of Science and Innovation of the Government of Spain and by the FEDER funds of the European Community through projects with codes TIN2017-84804-R, PID2020-112726-R and MTM2017-87162-P.

Appendix A. Probability density of the time between two events

The density function $f_T(t)$ of the time t elapsed between two events marked as arrhythmia by the system is derived in this appendix. Recall that we denote by $f(t|\lambda)$ the probability density function of an exponential distribution with rate parameter λ. $f(t|\lambda_1, \lambda_2)$ is the probability density function of a hypoexponential distribution with rates λ_1 and λ_2,

$$P(T_{AN} > t) = \int_t^{\infty} f(s|\lambda_{AN})ds \tag{5}$$

Let us assume, temporarily, that $\lambda_{AN} + \lambda_{AG} \neq \lambda_{NA}$. The probability distribution of the time between two events depends on the probability distributions of the elapsed time on each path, as follows:

$$f_T(t) = f(t|\lambda_{AG})P(T_{AN} > t) + \int_0^t f(s|\lambda_{AN})f(t-s|\lambda_{NA})P(T_{AG} > s)ds \tag{6}$$

Replacing the expressions of the density functions of the exponential densities and solving the integrals, we obtain that

$$f_T(t) = \lambda_{AG} e^{-\lambda_{AG} t} e^{-\lambda_{AN} t} + \int_0^t \lambda_{AN} e^{-\lambda_{AN} s} \lambda_{NA} e^{-\lambda_{NA}(t-s)} e^{-\lambda_{AG} s} ds == \lambda_{AG} e^{-\lambda_{AG} t} e^{-\lambda_{AN} t} + \lambda_{AN} \lambda_{NA} e^{-\lambda_{NA} t} \int_0^t e^{(\lambda_{NA} - \lambda_{AN} - \lambda_{AG}) s} ds == \lambda_{AG} e^{-\lambda_{AG} t} e^{-\lambda_{AN} t}$$
$$+ \frac{\lambda_{AN} \lambda_{NA}}{\lambda_{NA} - (\lambda_{AN} + \lambda_{AG})} e^{-\lambda_{NA} t} (e^{(\lambda_{NA} - \lambda_{AN} - \lambda_{AG}) t} - 1) == \lambda_{AG} e^{-(\lambda_{AG} + \lambda_{AN}) t} + \frac{\lambda_{AN} \lambda_{NA}}{\lambda_{NA} - (\lambda_{AN} + \lambda_{AG})} (e^{-(\lambda_{AN} + \lambda_{AG}) t} - e^{-\lambda_{NA} t}) =$$
$$= \frac{\lambda_{AG}}{\lambda_{AN} + \lambda_{AG}} (\lambda_{AN} + \lambda_{AG}) e^{-(\lambda_{AG} + \lambda_{AN}) t} + \frac{\lambda_{AN}}{\lambda_{AN} + \lambda_{AG}} \frac{(\lambda_{AN} + \lambda_{AG}) \lambda_{NA}}{\lambda_{NA} - (\lambda_{AN} + \lambda_{AG})} \cdot \quad \cdot (e^{-(\lambda_{AN} + \lambda_{AG}) t} - e^{-\lambda_{NA} t}) \tag{7}$$

and observing that $\lambda_A = \lambda_{AN} + \lambda_{AG}$, we conclude that the probability distribution of the time between two episodes is

$$f_T(t) = p_{AG} f(t|\lambda_A) + p_{AN} f(t|\lambda_A, \lambda_{NA}) \tag{8}$$

In the particular case that $\lambda_A = \lambda_{NA}$ (see Ref. [4]):

$$f(t|\lambda_A, \lambda_A) = \text{erlang}(t|\lambda_A) = \lambda_A^2 t e^{-\lambda_A t}. \tag{9}$$

Appendix B. Critical points of the likelihood function

Before studying the maximum likelihood estimate of the probability distribution in Eq. (8), we will study the case in which all the durations of the AF episodes are missing and all the paths are of type (T1), with no spurious exits. The solution of this particular case shows us that the likelihood function of the problem has more than one maximum and, therefore, it is necessary to resort to heuristics to initialize the EM algorithm. The general problem will be presented as a mixture of two distributions sharing a parameter.

The mean and the variance of a hypoexponential distribution with parameters λ_1, λ_2 are (see Ref. [4]):

$$\mu = \frac{1}{\lambda_1} + \frac{1}{\lambda_2}, \sigma^2 = \frac{1}{\lambda_1^2} + \frac{1}{\lambda_2^2} \tag{10}$$

and so, we have:

$$\frac{\sigma^2}{\mu^2} \in \left[\frac{1}{2}, 1\right] \tag{11}$$

Suppose that t_i $(i = 1, 2..., n)$, are i.i.d. with p.d.f.

$$f_{\text{hypo}}\left(t \middle| \lambda_1^*, \lambda_2^*\right) = \frac{\lambda_1^* \lambda_2^*}{\lambda_2^* - \lambda_1^*} \left(e^{-\lambda_1^* t} - e^{-\lambda_2^* t}\right) \tag{12}$$

we define the empirical log-likelihood function

$$\mathscr{L}_n(\lambda_1, \lambda_2) = \begin{cases} n(\log(\lambda_1) + \log(\lambda_2) \\ -\log\left(\lambda_1 - \lambda_2\right)\Big) + \sum_{i=1}^n \log\left(e^{-\lambda_1 t_i} - e^{-\lambda_2 t_i}\right) & \text{if} \quad \lambda_1 \neq \lambda_2 \\ 2n\lambda_1 + \sum_{i=1}^n \log(t_i) - \lambda_1 t_i & \text{if} \quad \lambda_1 = \lambda_2 \end{cases} \tag{13}$$

In the case $\lambda_1 \neq \lambda_2$, the necessary condition of a critical point is determined by:

$$0 = \frac{\partial \mathscr{L}_n}{\partial \lambda_1}(\lambda_1, \lambda_2) = \frac{n}{\lambda_1} + \frac{n}{\lambda_2 - \lambda_1} + \sum_{i=1}^n \frac{-t_i e^{-\lambda_1 t_i}}{e^{-\lambda_1 t_i} - e^{-\lambda_2 t_i}} \tag{14}$$

$$0 = \frac{\partial \mathscr{L}_n}{\partial \lambda_2}(\lambda_1, \lambda_2) = \frac{n}{\lambda_2} - \frac{n}{\lambda_2 - \lambda_1} + \sum_{i=1}^n \frac{t_i e^{-\lambda_2 t_i}}{e^{-\lambda_1 t_i} - e^{-\lambda_2 t_i}} \tag{15}$$

Adding (14) and (15), we have:

$$\frac{1}{\lambda_1} + \frac{1}{\lambda_2} = \frac{\sum_{i=1}^n t_i}{n} = \mu_n \underset{n \to \infty}{\longrightarrow} \mu^* \tag{16}$$

This equality implies that any critical point belongs to a curve. Furthermore, the symmetry of the hypoexponential distribution implies that we always have a critical point in $\frac{1}{\lambda_1} = \frac{1}{\lambda_2} = \frac{\sum_{i=1}^n t_i}{2n}$. A direct computation implies that this point is a local maximum in the case $\sigma_n^2 < \frac{\mu_n^2}{2}$ where σ_n^2 denotes the empirical variance. This symmetrical critical point is a saddle point in the more natural case $\sigma_n^2 > \frac{\mu_n^2}{2}$ (see Appendix C). Therefore, in this simplified problem, it is expected that the empirical log-likelihood function will have more than one critical point.

We have not been able to prove the existence of two symmetric global maximums of the empirical log-likelihood function, but the numerical simulations indicate that, on the restriction given by (16), we have two local maximums that converge to the two symmetrical theoretical values when the number of samples is large enough.

It must be said that the symmetry of the p.d.f. of the hypoexponential distribution implies that we cannot use the usual arguments of consistency of the maximum likelihood estimator because we have an identification problem (see Appendix D). The possible existence of more than one critical point of the empirical log-likelihood with finite-sized samples, induces us to use a heuristic algorithm to find a starting point at which to apply the method of expectation maximization in order to estimate the parameters of the distribution.

An EM algorithm is defined In Appendix E for the particular case where all durations are unknown and all paths are of type (T1), with no spurious exits, as mentioned above. The solution of the general case is addressed in Appendix F.

Appendix C. Critical point character in the hypoexponential case

The symmetrical critical point is a saddle point in the more natural case $\sigma_n^2 > \frac{\mu_n^2}{2}$:

$$\frac{\partial^2}{\partial\lambda_1^2}\mathscr{L}_n(\lambda,\lambda) = \frac{\partial^2}{\partial\lambda_1^2}\mathscr{L}_n(\lambda,\lambda) = -\frac{1}{\lambda^2} + \frac{1}{12n}\sum_{i=1}^{n} x_i^2 \tag{17}$$

$$\frac{\partial^2}{\partial\lambda_1\partial\lambda_2}\mathscr{L}_n(\lambda,\lambda) = -\frac{1}{12n}\sum_{i=1}^{n} x_i^2 \tag{18}$$

and the Hessian:

$$H\mathscr{L}_n(\lambda,\lambda) = -\frac{1}{\lambda^4} + \frac{1}{6\lambda^2 n}\sum_{i=1}^{n} x_i^2 \tag{19}$$

If $\lambda = \frac{2}{\mu_n}$ then

$$H\mathscr{L}_n(\lambda,\lambda) > 0 \Leftrightarrow \frac{\sum_{i=1}^{n} x_i^2}{n\mu_n^2} > \frac{3}{2} \Leftrightarrow \frac{\sigma_n^2}{\mu_n^2} > \frac{1}{2} \tag{20}$$

Appendix D. Consistency of the estimation in the hypoexponential case

Adding equation (14) multiplied by $\frac{1}{\lambda_1}$ and equation (15) multiplied by $\frac{1}{\lambda_2}$, we have:

$$\frac{1}{\lambda_1^2} + \frac{1}{\lambda_2^2} + \frac{1}{\lambda_1\lambda_2} = \frac{1}{n}\sum_{i=1}^{n} \frac{\frac{1}{\lambda_1} t_i e^{-\lambda_1 t_i} - \frac{1}{\lambda_2} t_i e^{-\lambda_2 t_i}}{e^{-\lambda_1 t_i} - e^{-\lambda_2 t_i}} \tag{21}$$

The right hand side of (21) is not equal to $\sigma_n^2 + \frac{1}{\lambda_1\lambda_2}$. But if we evaluate (21) in the theoretical values $(\lambda_1^*, \lambda_2^*)$, the law of large numbers implies that the right hand side in (21) converges when the size of the sample incresases, to:

$$\begin{aligned}\int_0^\infty t\left(\frac{1}{\lambda_1^*} t e^{-\lambda_1^* t} - \frac{1}{\lambda_2^*} t_i e^{-\lambda_2^* t}\right) \frac{\lambda_1^*\lambda_2^*}{\lambda_2^* - \lambda_1^*} \frac{e^{-\lambda_1^* t} - e^{-\lambda_2^* t}}{e^{-\lambda_1^* t} - e^{-\lambda_2^* t}} dt = \\ = \frac{1}{\lambda_1^{*2}} + \frac{1}{\lambda_2^{*2}} + \frac{1}{\lambda_1^*\lambda_2^*}\end{aligned} \tag{22}$$

so

$$\lim_{n\to\infty} \frac{\partial\mathscr{L}_n}{\partial\lambda_i}(\lambda_1^*, \lambda_2^*) = 0, i = 1, 2 \tag{23}$$

which implies the consistency of the estimation.

Appendix E. Expectation-maximization estimation in the hypoexponential distribution

In this case, the observed values are t_i, the sum of the intermediate times. We will consider the first intermediate time x_i as the hidden variable and $\theta = (\lambda_1, \lambda_2)$ as the parameters.

We denote by

$$\mathscr{L}_n^{(m)}(\theta) = \frac{1}{n}\sum_{i=1}^{n} \int_0^{t_i} f(x|t_i, \theta^{(m)}) log(f(x, t_i|\theta)) dt \tag{24}$$

where $\theta = (\lambda_1, \lambda_2)$,

$$f(x, t_i|\theta) = \lambda_1 e^{-\lambda_1 x} \lambda_2 e^{-\lambda_2 (t_i - x)} \tag{25}$$

$$f(x|t_i, \theta) = \frac{f(x, t_i|\theta)}{f_{\text{hypo}}(t_i|\theta)} \tag{26}$$

In the Expectation-Maximization algorithm (EM), for any m, we obtain new parameters $\theta^{(m+1)} = (\lambda_1^{(m+1)}, \lambda_2^{(m+1)})$ that maximize the concave function $\mathscr{L}_n^{(m+1)}$.

If we define:

$$\beta_{i1}^{(m)} = \frac{1}{f_{\text{hypo}}(t_i|\theta^{(m)})} \int_0^{t_i} e^{-\lambda_1^{(m)} x} e^{-\lambda_2^{(m)}(t_i - x)} x dx \tag{27}$$

and

$$\beta_{i2}^{(m)} = \frac{1}{f_{\text{hypo}}(t_i|\theta^{(m)})} \int_0^{t_i} e^{-\lambda_1^{(m)} x} e^{-\lambda_2^{(m)}(t_i - x)} (t_i - x) dx \tag{28}$$

then the algorithm consists in computing, from the given initial values $\theta^{(0)} = (\lambda_1^{(0)}, \lambda_2^{(0)})$ and for any m:

$$\frac{1}{\lambda_1^{(m+1)}} = \frac{1}{n} \sum_{i=1}^{n} \beta_{i1}^{(m)} \tag{29}$$

$$\frac{1}{\lambda_2^{(m+1)}} = \frac{1}{n} \sum_{i=1}^{n} \beta_{i2}^{(m)} \tag{30}$$

It is not feasible to make a strong imputation of the value of the intermediate time for a given final time because

$$\frac{\partial \log(f(x, t_i|\theta))}{\partial x} = \lambda_2 - \lambda_1 \tag{31}$$

and therefore an intermediate time could not be selected.

Appendix F. Expected maximization estimation in the general case

The density function is:

$$\begin{aligned} & f(t|\tau, \lambda_1, \lambda_2) = \\ & = \tau f_{\text{exp}}(t|\lambda_1) + (1 - \tau) f_{\text{hypo}}(t|\lambda_1, \lambda_2) = \\ & = \tau \lambda_1 e^{-\lambda_1 t} + (1 - \tau) \frac{\lambda_1 \lambda_2}{\lambda_2 - \lambda_1} (e^{-\lambda_1 t} - e^{-\lambda_2 t}) \end{aligned} \tag{32}$$

if $\lambda_1 \neq \lambda_2$. In the other case, we must replace the hypoexponential distribution for the Erlang distribution. This distribution can be interpreted as the mixture of an exponential distribution and a hypoexponential distribution with a shared parameter.

In order to apply the EM algorithm to estimate the parameters of this distribution, we will consider as hidden variables:

- times t_i in the sample, that can be of types T1 or T2 (recall Eqs. (2) and (3)).
- the AF episode length, when t_i comes from the hypoexponential distribution.

The parameters are $\theta = (\tau, \lambda_1, \lambda_2)$. We define the functions that follow:

$$\begin{aligned} & \mathscr{L}_n^{(m)}(\tau, \lambda_1, \lambda_2) = \\ & \frac{1}{n} \sum_{i=1}^{n} \left(p\left(z_i = 1|t_i, \theta^{(m)} \right) \log\left(f(z_i = 1, t_i|\theta \right) + + \int_0^{t_i} f\left(z_i = 2, x|t_i, \theta^{(m)} \right) \log\left(f(z_i = 2, x, t_i|\theta \right) \right) dt \right) \end{aligned} \tag{33}$$

where

$$\begin{aligned} & p(z_i = 1|t_i, \theta^{(m)}) = \\ & \frac{f(z_i = 1, t_i|\theta^{(m)})}{f(t_i|\theta^{(m)})} = \\ & \frac{\tau f_{\text{exp}}\left(t_i|\theta^{(m)}\right))}{\tau^{(m)} f_{\text{exp}}\left(t_i|\theta^{(m)}\right)) + (1 - \tau^{(m)}) f_{\text{hypo}}(t_i|\theta^{(m)})} := \Gamma_{i1}^{(m)} \end{aligned} \tag{34}$$

and

$$f(z_i = 2, x|t_i, \theta^{(m)}) = \frac{f(z_i = 2, x, t_i|\theta^{(m)})}{f(t_i|\theta^{(m)})} = \frac{\left(1-\tau^{(m)}\right) f_{\exp}\left(x|\lambda_1^{(m)}\right) f_{\exp}\left(t_i - x|\ \lambda_2^{(m)}\right)}{\tau^{(m)} f_{\exp}\left(t_i|\theta^{(m)}\right)) + \left(1-\tau^{(m)}\right) f_{\text{hypo}}\left(t_i|\theta^{(m)}\right)} := \gamma_{i2}^{(m)}\left(x\right) \tag{35}$$

Finally,

$$\log(f(z_i = 1, t_i|\theta)) = \log(\tau) + \log(\lambda_1) - \lambda_1 t_i \tag{36}$$

and

$$\log(f(z_i = 2, x, t_i|\theta)) = \log(1-\tau) + \log(\lambda_1) - \lambda_1 t_i + \log(\lambda_2) - \lambda_2(t_i - x) \tag{37}$$

satisfying

$$\Gamma_{i1}^{(m)} + \int_0^{t_i} \gamma_{i2}^{(m)}(x)dx := \Gamma_{i1}^{(m)} + \Gamma_{i2}^{(m)} = 1. \tag{38}$$

Functions $\mathscr{L}_n^{(m)}$ are concave and therefore have a single maximum (See Appendix G).

If we define:

$$\beta_{i1}^{(m)} = \int_0^{t_i} \gamma_{i2}^{(m)}(x)xdx, \tag{39}$$

$$\beta_{i2}^{(m)} = \int_0^{t_i} \gamma_{i2}^{(m)}(x)(t_i - x)dx \tag{40}$$

then the algorithm consists in computing, from the given initial values $\theta^{(0)} = (\tau^{(0)}, \lambda_1^{(0)}, \lambda_2^{(0)})$ and for any m:

$$\frac{1}{\lambda_1^{(m+1)}} = \frac{1}{n}\sum_{i=1}^{n} \Gamma_{i1}^{(m)} t_i + \beta_{i1}^{(m)} \tag{41}$$

$$\frac{1}{\lambda_2^{(m+1)}} = \frac{\sum_{i=1}^{n} \beta_{i2}^{(m)}}{\sum_{i=1}^{n} \Gamma_{i2}^{(m)}} \tag{42}$$

$$\tau = \frac{\frac{1}{\sum_{i=1}^{n} \Gamma_{i2}^{(m)}}}{\frac{1}{\sum_{i=1}^{n} \Gamma_{i1}^{(m)}} + \frac{1}{\sum_{i=1}^{n} \Gamma_{i2}^{(m)}}} \tag{43}$$

In the case where there is an AF episode length for an interval t_i, we can replace the corresponding terms in the EM estimations.

Observe also that when the duration x_i equals the time interval t_i, then we have a false exit and have to consider the values:

$$\Gamma_{i1}^{(m)} = 1,\ \Gamma_{i2}^{(m)} = \beta_{i1}^{(m)} = \beta_{i2}^{(m)} = 0. \tag{44}$$

if the duration is shorter than the time interval, then we impose the values

$$\Gamma_{i1}^{(m)} = 0,\ \Gamma_{i2}^{(m)} = 1,\ \beta_{i1}^{(m)} = x_i,\ \beta_{i2}^{(m)} = t_i - x_i. \tag{45}$$

F.1 Local convergence of the EM algorithm

In [25] the authors prove that under some conditions the EM algorithm converges to a critical point of the empirical likelihood and if the unique critical point is a global maximum the algorithm converges to this maximum.

In our case it is impossible to be certain that the empirical likelihood function has a unique critical point. The existence of the unique maximum is a consequence of the identification property (See Appendix H).

Appendix G. Concavity of $\mathscr{L}_{\mathbf{n}}^{(\mathbf{m})}$ in the interior of the domain

Observe that

$$\frac{\partial^2}{\partial\tau^2}\mathscr{L}_n^{(m)}(\tau,\lambda_1,\lambda_2) = -\frac{1}{n\tau^2}\sum_{i=1}^{n}\Gamma_{i1}^{(m)} - \frac{1}{n(1-\tau)^2}\sum_{i=1}^{n}\Gamma_{i2}^{(m)} \tag{46}$$

$$\frac{\partial^2}{\partial\lambda_1^2}\mathscr{L}_n^{(m)}(\tau,\lambda_1,\lambda_2) = -\frac{1}{\lambda_1^2} \tag{47}$$

$$\frac{\partial^2}{\partial\lambda_2^2}\mathscr{L}_n^{(m)}(\tau,\lambda_1,\lambda_2) = -\frac{1}{n\lambda_2^2}\sum_{i=1}^{n}\Gamma_{i2}^{(m)} \tag{48}$$

and the mixed partial derivatives are zero.

Appendix H. Identification of the distribution in the general case

Given

$$f(\tau,\lambda_1,\lambda_2) = (1-\tau)e^{-\lambda_1 x} + \tau\frac{\lambda_1\lambda_2}{\lambda_2-\lambda_1}(e^{-\lambda_1 x} - e^{\lambda_2 x}) \tag{49}$$

we want to prove that there are no two parameters $\tau^{'}$, $\lambda_1{}^{'}$, $\lambda_2{}^{'}$ with the same value functions:

$$f(\tau,\lambda_1,\lambda_2) = f(\tau^{'},\lambda_1{}^{'},\lambda_2{}^{'}) \tag{50}$$

The independence of exponential functions indicates that the only two possibilities are:

1. $\lambda_1 = \lambda_1{}^{'}, \lambda_2 = \lambda_2{}^{'}$
2. $\lambda_1 = \lambda_2{}^{'}, \lambda_2 = \lambda_1{}^{'}$

In the first case, clearly $\tau = \tau^{'}$. In the second case, given the antisymmetry of $\frac{\lambda_1\lambda_2}{\lambda_2-\lambda_1}$ and using the notation $\lambda = \frac{\lambda_1\lambda_2}{\lambda_2-\lambda_1}$ we see that:

$$(1-\tau) + \tau\lambda = \tau^{'}\lambda \tag{51}$$

$$-\tau\lambda = 1 - \tau^{'} - \tau^{'}\lambda \tag{52}$$

The determinant of the system of equations with variables τ, $\tau^{'}$ is

$$\begin{vmatrix} \lambda-1 & -\lambda \\ -\lambda & 1+\lambda \end{vmatrix} = -1 \tag{53}$$

and their solutions are unique $\tau = \tau^{'} = 1$, so we have the hypoexponential case.

Appendix I. Local Convergence

Considering the auxiliary function $f_i(\lambda_1 - \lambda_2) = \frac{1}{\lambda_2-\lambda_1}(1 - e^{(\lambda 1-\lambda_2)t_i})$, the partial derivatives of the likelihood function are:

$$0 = \frac{\partial\mathscr{L}_n}{\partial\tau}(\tau,\lambda_1,\lambda_2) = \sum_{i=1}^{n}\frac{1-\lambda_2 f_i(\lambda_1-\lambda_2)}{\tau+(1-\tau)\lambda_2 f_i(\lambda_1-\lambda_2)} \tag{54}$$

$$0 = \frac{\partial\mathscr{L}_n}{\partial\lambda_1}(\tau,\lambda_1,\lambda_2) = = \frac{n}{\lambda_1} + \sum_{i=1}^{n}t_i + \sum_{i=1}^{n}\frac{(1-\tau)\lambda_2 f_i^{'}(\lambda_1-\lambda_2)}{\tau+(1-\tau)\lambda_2 f_i(\lambda_1-\lambda_2)} \tag{55}$$

$$0 = \sum_{i=1}^{n}\frac{(1-\tau)(-\lambda_2 f_i^{'}(\lambda_1-\lambda_2) + f_i((\lambda_1-\lambda_2))}{\tau+(1-\tau)\lambda_2 f_i(\lambda_1-\lambda_2)} \tag{56}$$

From (54) we can define

$$\mu := \sum_{i=1}^{n}\frac{1}{\tau+(1-\tau)\lambda_2 f_i(\lambda_1-\lambda_2)} = = \sum_{i=1}^{n}\frac{\lambda_2 f_i(\lambda_1-\lambda_2)}{\tau+(1-\tau)\lambda_2 f_i(\lambda_1-\lambda_2)} \tag{57}$$

however,

$$\mu = \tau\mu + (1-\tau)\mu = \\ = \sum_{i=1}^{n} \frac{\tau}{\tau + (1-\tau)\lambda_2 f_i(\lambda_1 - \lambda_2)} + \\ + \sum_{i=1}^{n} \frac{(1-\tau)\lambda_2 f_i(\lambda_1 - \lambda_2)}{\tau + (1-\tau)\lambda_2 f_i(\lambda_1 - \lambda_2)} = n \tag{58}$$

thus,

$$\frac{1}{n}\sum_{i=1}^{n} \frac{f_i(\lambda_1 - \lambda_2)}{\tau + (1-\tau)\lambda_2 f_i(\lambda_1 - \lambda_2)} = \frac{1}{\lambda_2} \tag{59}$$

Finally, summing (55) and (56) and using (59) we obtain that the mean of the maximum likelihood distribution is equal to the sample mean:

$$\frac{1}{\lambda_2} + (1-\tau)\frac{1}{\lambda_2} = \frac{1}{n}\sum_{i=1}^{n} t_i \tag{60}$$

Appendix J. Heuristics for initializing the EM algorithm

The EM algorithm has local convergence to one of the critical points but we cannot guarantee the existence of a unique critical point that is a global maximum. The EM must be started from a set of coefficients that allow a strong imputation of the interval type for each of the sample intervals. Two different initializations are considered:

J.1 Heuristic without durations

This initializacion consists in a simplified likelihood function where τ is a variable. The intervals are sorted first, according to their lengths. For each value of τ the sorted list is divided into two groups. The mean of the durations of the group with shorter lengths is used to obtain an initial value for $\frac{1}{\lambda 1}$ and the mean of the remaining data is used for estimating $\frac{1}{\lambda 1} + \frac{1}{\lambda 2}$. The value of τ that maximizes the likelihood of these two assignments is chosen.

J.2 Heuristic with durations

The intervals between two AMS events are categorized as follows:

1. Intervals whose length is much lower than the AF episode length. These intervals are assigned the type T1 (Positive → True Negative → Positive).
2. Intervals whose length is of the same order as the AF episode. These episodes are assigned the type T2 (Positive → Positive)
3. Intervals without known AF episode length: these episodes are sorted and a duration d is selected. Intervals shorter than d are imputed as type T2 and intervals longer than d are imputed as type T1.

For each value of d, λ_1 and λ_2 are estimated for the three categories:

1. Type T1 with AF duration: the mean of the durations is an estimation of $\frac{1}{\lambda_1}$ and the mean of the interval lengths minus the AF length is an estimation of $\frac{1}{\lambda_2}$.
2. Type T2 with AF duration: the mean of the interval lengths is an estimation of $\frac{1}{\lambda_1}$.
3. Intervals without AF duration: the heuristic without durations mentioned before is applied

The initial estimation of $\frac{1}{\lambda_1}$ and $\frac{1}{\lambda_2}$ is obtained as a weighted mean of the different estimations, with weights proportional to the number of samples involved at each estimation. The value of d that maximizes the posterior likelihood is chosen.

References

[1] C.C. Aggarwal, Data Classification: Algorithms and Applications, first ed., Chapman & Hall/CRC, 2014.

[2] M.I. Alhusseini, F. Abuzaid, A.J. Rogers, J.A. Zaman, T. Baykaner, P. Clopton, P. Bailis, M. Zaharia, P.J. Wang, W.-J. Rappel, et al., Machine learning to classify intracardiac electrical patterns during atrial fibrillation: machine learning of atrial fibrillation, Circulation: Arrhythmia Electrophysiol. 13 (8) (2020), e008160.

[3] J.A. Bilmes, et al., A Gentle Tutorial of the Em Algorithm and its Application to Parameter Estimation for Gaussian Mixture and Hidden Markov Models, 1998.

[4] G. Bolch, S. Greiner, H. De Meer, K.S. Trivedi, Queueing Networks and Markov Chains: Modeling and Performance Evaluation with Computer Science Applications, John Wiley & Sons, 2006.

[5] D. Calvo, D. Filgueiras-Rama, J. Jalife, Mechanisms and drug development in atrial fibrillation, Pharmacol. Rev. 70 (3) (2018) 505–525.

[6] N. Costa, J. Fernández, I. Couso, L. Sánchez, Graphical analysis of the progression of atrial arrhythmia using recurrent neural networks, Int. J. Comput. Intell. Syst. 13 (1) (2020) 1567–1577.

[7] I. Couso, D. Dubois, E. Hüllermeier, Maximum likelihood estimation and coarse data, in: International Conference on Scalable Uncertainty Management, Springer, 2017, pp. 3–16.

[8] J. Fernández, L. Sánchez, D. Calvo, J. Velasco, Correction of Pacemaker Mode Switch Episodes, Elsevier, 2021, https://doi.org/10.17632/tfpyywh46w.1. Mendeley Data.

[9] T.V. Glotzer, E.G. Daoud, D.G. Wyse, D.E. Singer, M.D. Ezekowitz, C. Hilker, C. Miller, D. Qi, P.D. Ziegler, The relationship between daily atrial tachyarrhythmia burden from implantable device diagnostics and stroke risk: the TRENDS study, Circulation: Arrhythmia Electrophysiol. 2 (5) (2009) 474–480.

[10] M.R. Gold, Treatment of subclinical atrial fibrillation: does one plus one always equal two? Circulation 137 (3) (2018) 217–218.

[11] R. Guillaume, I. Couso, D. Dubois, Maximum Likelihood with Coarse Data Based on Robust Optimisation, 2017.

[12] D.F. Heitjan, D.B. Rubin, Ignorability and Coarse Data, The annals of statistics, 1991, pp. 2244–2253.

[13] G. Hindricks, T. Potpara, N. Dagres, E. Arbelo, J.J. Bax, C. Blomström-Lundqvist, G. Boriani, M. Castella, G.-A. Dan, P.E. Dilaveris, et al., ESC guidelines for the diagnosis and management of atrial fibrillation, Eur. Heart J. 2020 (2020).

[14] E. Hüllermeier, S. Destercke, I. Couso, Learning from imprecise data: adjustments of optimistic and pessimistic variants, in: International Conference on Scalable Uncertainty Management, Springer, 2019, pp. 266–279.
[15] E.S. Kaufman, C.W. Israel, G.M. Nair, L. Armaganijan, S. Divakaramenon, G. H. Mairesse, A. Brandes, E. Crystal, O. Costantini, R.K. Sandhu, et al., Positive predictive value of device-detected atrial high-rate episodes at different rates and durations: an analysis from assert, Heart Rhythm 9 (8) (2012) 1241–1246.
[16] R. Mahajan, T. Perera, A.D. Elliott, D.J. Twomey, S. Kumar, D.A. Munwar, K. B. Khokhar, A. Thiyagarajah, M.E. Middeldorp, C.J. Nalliah, et al., Subclinical device-detected atrial fibrillation and stroke risk: a systematic review and meta-analysis, Eur. Heart J. 39 (16) (2018) 1407–1415.
[17] R. Mahajan, T. Perera, A.D. Elliott, D.J. Twomey, S. Kumar, D.A. Munwar, K. B. Khokhar, A. Thiyagarajah, M.E. Middeldorp, C.J. Nalliah, J.M.L. Hendriks, J. M. Kalman, D.H. Lau, P. Sanders, Subclinical device-detected atrial fibrillation and stroke risk: a systematic review and meta-analysis, Eur. Heart J. 39 (16) (01 2018) 1407–1415.
[18] A.A. Markov, Extension of the limit theorems of probability theory to a sum of variables connected in a chain, Dynam. Probabilistic Syst. 1 (1971) 552–577.
[19] B. Mor, S. Garhwal, A. Kumar, A systematic review of hidden markov models and their applications, Arch. Comput. Methods Eng. (2020), https://doi.org/10.1007/s11831-020-09422-4.
[20] W.M. Pollak, J.D. Simmons, A. Interian Jr., S.A. Atapattu, A. Castellanos, R. J. Myerburg, R.D. Mitrani, Clinical utility of intraatrial pacemaker stored electrograms to diagnose atrial fibrillation and flutter, Pacing Clin. Electrophysiol. 24 (4) (2001) 424–429.
[21] J.S. Steinberg, H. O'Connell, S. Li, P.D. Ziegler, Thirty-second gold standard definition of atrial fibrillation and its relationship with subsequent arrhythmia patterns: analysis of a large prospective device database, Circulation: Arrhythmia Electrophysiol. 11 (7) (2018), e006274.
[22] C.D. Swerdlow, M.L. Brown, P. Bordachar, Sensing and detection with cardiac implantable electronic devices, in: Clinical Cardiac Pacing, Defibrillation and Resynchronization Therapy, Elsevier, 2017, pp. 114–167.
[23] I.C. Van Gelder, J.S. Healey, H.J. Crijns, J. Wang, S.H. Hohnloser, M.R. Gold, A. Capucci, C.-P. Lau, C.A. Morillo, A.H. Hobbelt, M. Rienstra, S.J. Connolly, Duration of device-detected subclinical atrial fibrillation and occurrence of stroke in ASSERT, Eur. Heart J. 38 (17) (03 2017) 1339–1344.
[24] N.E. Wineinger, P.M. Barrett, Y. Zhang, I. Irfanullah, E.D. Muse, S.R. Steinhubl, E. J. Topol, Identification of paroxysmal atrial fibrillation subtypes in over 13,000 individuals, Heart Rhythm 16 (1) (2019) 26–30.
[25] C.J. Wu, On the convergence properties of the em algorithm, Ann. Stat. (1983) 95–103.